

## Angular Distributions of $1s\sigma$ Photoelectrons from Fixed-in-Space $N_2$ Molecules

E. Shigemasa, J. Adachi,\* M. Oura,† and A. Yagishita

Photon Factory, National Laboratory for High Energy Physics, Oho 1-1, Tsukuba-shi, Ibaraki-ken 305, Japan  
(Received 27 June 1994)

The angular distributions of  $1s\sigma$  photoelectrons from  $N_2$  molecules held fixed in space have been measured around the  $\sigma^*$  shape resonance for the first time. The angular distributions have been very rich in structure, which are completely different from usual photoelectron angular distributions from randomly oriented molecules, as predicted by Dill. The orbital angular momentum properties of the  $1s\sigma$  photoelectrons around the  $\sigma^*$  shape resonance have been made clear from the angular distribution patterns.

PACS numbers: 33.80.Eh, 33.90.+h

Molecular  $K$ -shell spectra are known to depart remarkably from corresponding atomic spectra [1]. Specifically, above the  $K$  edge there is a broad band of enhanced photoabsorption in place of the smooth monotonic decrease one might expect. The novel feature, so called shape resonance, results from the interaction between the photoelectron escaping from the  $K$  shell and the anisotropic molecular field [2].

Direct study of the orbital angular momentum properties of the photoelectrons in the shape resonance is not possible by conventional gas-phase photoelectron angular distribution studies, owing to the random orientations of the molecules. If, however, the molecules have a definite orientation, the angular distributions of photoelectrons ejected by the electric-dipole interaction has the general form [3]

$$\frac{d\sigma}{d\Omega} = \sum_{K=0}^{2l_{\max}} \sum_M A_{KM} Y_{KM}(\theta, \phi), \quad (1)$$

where the angles  $\{\theta, \phi\}$  are measured from the molecule  $z$  axis,  $l_{\max}$  is the maximum orbital angular momentum component of the outgoing photoelectron, and  $Y_{KM}$  are the spherical harmonics. Thus, such photoelectron angular distributions of fixed-in-space molecules can offer a direct probe of the orbital angular momentum composition of the molecular photoelectrons. In the limited case, the angular distribution of photoelectrons from oriented  $H_2$  [4], CO [5], and  $N_2$  and CO [6] molecules were predicted by three groups.

The present experiment has been undertaken to study the orbital angular momentum properties of the photoelectrons in a prototype molecular shape resonance—the  $\sigma^*$  shape resonance of nitrogen molecules. In this Letter, we present the first experimental results on the angular distributions of  $1s\sigma$  photoelectrons ejected from  $N_2$  molecules held fixed in space. The photoionization processes of fixed-in-space molecules in a gas phase can be realized by detecting photoelectrons in coincidence with fragment ions as reported by Golovin *et al.* [7,8]. Since the dissociation time of the molecular ions produced by a subsequent Auger decay of the  $K$ -shell vacancy is much shorter than the molecular rotation period, the emission

direction of the fragment ion is considered to be equivalent to the molecular orientation at a moment of absorption of a photon.

The experiments have been carried out on beam line BL-2B, supplying the synchrotron radiation emitted from an undulator [9] inserted in the 2.5 GeV positron storage ring at the Photon Factory. The undulator radiation, monochromatized with a 10 m grazing incidence monochromator [10], was focused onto an effusive beam of the sample gas at the center of the ionization region of the experimental chamber. The entrance and exit slit openings of the monochromator were both set to 50  $\mu\text{m}$ . The expected energy resolution was about 0.6 eV at  $h\nu = 400$  eV. The diameter of the photon beam spot at the sample position was less than 0.2 mm. The first harmonic of the undulator radiation was used for all measurements described here. It had been confirmed in our previous work that the degree of linear polarization within the first harmonic peak of the undulator radiation is more than 95% [11]. Two identical ion detectors (channeltrons) with retarding grids were installed in the chamber at  $0^\circ$  and  $90^\circ$  relative to the polarization vector of the incident radiation in the plane perpendicular to the radiation path. A retarding potential of +3 V was applied to the grid of each detector to select energetic fragment ions only. Each detector has a collection half-angle of  $10.5^\circ$ . A parallel plate electrostatic analyzer with a position sensitive detector (a microchannel plate and a resistive anode), which can be rotated around the photon beam axis, was used to energy analyze photoelectrons [11]. The effective acceptance angle of the analyzer was estimated to be  $\pm 5^\circ$ . To obtain coincidence signals between photoelectrons and fragment ions, event signals from the electron detector were fed into two time-to-amplitude converters to start them at the same time, and signals from one ion detector were used to stop one of the converters and signals from the other detector to stop the other.

As demonstrated in our previous work [11–19], the energetic fragment-ion angular distributions after the  $K$ -shell excitations of diatomic molecules induced by linearly polarized radiation have enabled us to decompose the conventional photoabsorption spectra into their molecular

symmetry components not only at the discrete resonances but also in the continuum states. Above the  $K$ -shell ionization threshold of  $N_2$ , the signal intensities of the fragment ions ( $N^+$  or  $N^{2+}$ ) emitted parallel to the electric vector of the incident light provide the strength of parallel transitions ( $1s\sigma_{g,u} \rightarrow \varepsilon\sigma_{u,g}$  ionization channels), while the intensities of the ions emitted perpendicular to the vector give the strength of perpendicular transitions ( $1s\sigma_{g,u} \rightarrow \varepsilon\pi_{u,g}$  ionization channels). The angular dependence of the coincidence signals between the photoelectrons and the fragment ions detected by the  $0^\circ$  ion detector yields the angular distributions of the photoelectrons from the molecules oriented parallel to the electric vector of the incident light, while that between the photoelectrons and the ions detected by the  $90^\circ$  detector produces the angular distributions of the photoelectrons from the molecules oriented perpendicular to the vector.

The angular distribution patterns of the  $1s\sigma$  photoelectrons for the parallel transitions, at three different photon energies, are shown in Fig. 1 and the patterns for the perpendicular transitions are presented in Fig. 2. The experimental data points are represented by filled circles with error bars, and the solid curves show the theoretical ones fitted to the experimental data using the least-squares method, whose procedure will be described later. In each graph, the maximum value is normalized to unity. It should be noted that  $\theta$  is the photoelectron ejection angle measured from the molecular axis. As is clearly

seen in Figs. 1 and 2, the observed angular distributions are very rich in structure, which are completely different from usual photoelectron angular distributions from randomly oriented molecules expressed as the functional form of  $1 + \beta P_2(\cos\theta')$ , where  $\beta$  is the asymmetry parameter, and  $\theta'$  is measured from the electric vector of the light. And they also show dramatic spectral variation of the fixed-molecule photoelectron angular distributions.

In order to analyze the present results quantitatively, we have used the formula of Dill for the fixed-molecule photoelectron angular distributions [3]. The general result expressed by Eq. (1) can be simplified for the special case, i.e., the photoionization of cylindrically symmetric molecules with the electric vector parallel or perpendicular to the molecule  $z$  axis. In this case, the differential cross section (1) becomes

$$\frac{d\sigma}{d\hat{k}} = \sum_{K=0}^{2l_{\max}} A_K P_K(\cos\theta), \quad (2)$$

where  $\hat{k} = \{\theta, 0\}$  is the photoelectron ejection direction measured in the molecule frame, and  $P_K$  is the Legendre polynomials. In the  $1s\sigma$  photoionization channels of  $N_2$  molecules, we take account of four dominant channels for the parallel transitions, i.e.,  $1s\sigma_g \rightarrow p\sigma_u, f\sigma_u$  and  $1s\sigma_u \rightarrow s\sigma_g, d\sigma_g$ , and three dominant channels for the perpendicular transitions, i.e.,  $1s\sigma_g \rightarrow p\pi_u, f\pi_u$ , and  $1s\sigma_u \rightarrow d\pi_g$ . Under these considerations, the expansion coefficients  $A_K$  of the Legendre polynomials of Eq. (2)

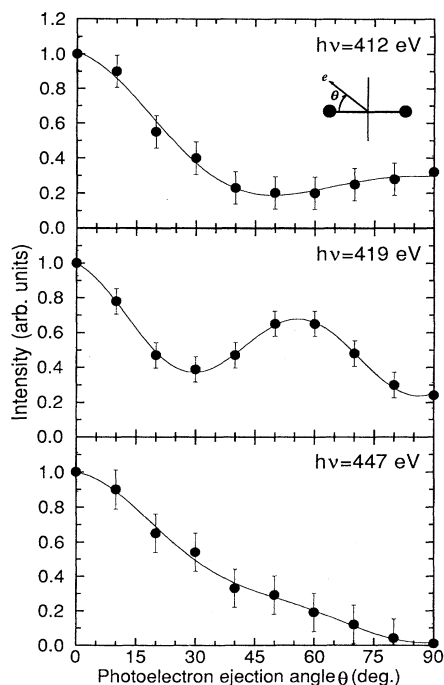


FIG. 1. Angular distributions of  $1s\sigma$  photoelectrons from  $N_2$  molecules oriented parallel to the electric vector of the incident light. The filled circles with error bars represent experimental data points, and the solid curves show the theoretical ones fitted to the experimental data (see text).

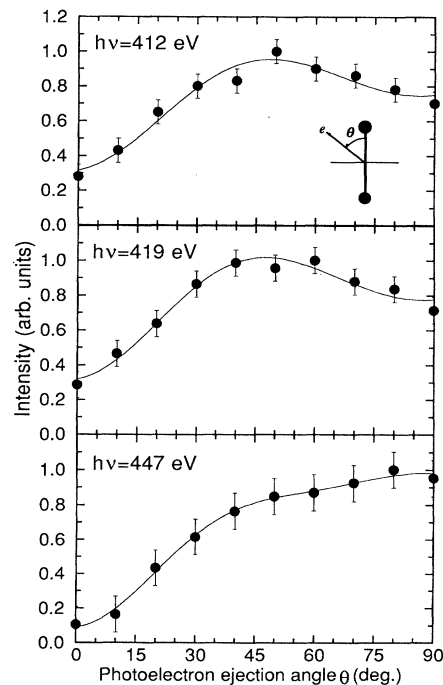


FIG. 2. Angular distributions of  $1s\sigma$  photoelectrons from  $N_2$  molecules oriented perpendicular to the electric vector of the incident light. The filled circles with error bars represent experimental data points, and the solid curves show the theoretical ones fitted to the experimental data.

may be written for the parallel transitions by

$$\begin{aligned}
 A_0'' &= \pi\alpha h\nu(|D_{s\sigma}|^2 + |D_{p\sigma}|^2 + |D_{d\sigma}|^2 + |D_{f\sigma}|^2), \\
 A_2'' &= \pi\alpha h\nu\left(2|D_{p\sigma}|^2 + \frac{10}{7}|D_{d\sigma}|^2 + \frac{4}{3}|D_{f\sigma}|^2\right. \\
 &\quad \left.- 2\sqrt{5}D_{s\sigma}^*D_{d\sigma}\cos\Delta_{sd}\right. \\
 &\quad \left.- 6\sqrt{\frac{3}{7}}D_{f\sigma}^*D_{p\sigma}\cos\Delta_{pf}\right), \\
 A_4'' &= \pi\alpha h\nu\left(\frac{18}{7}|D_{d\sigma}|^2 + \frac{18}{11}|D_{f\sigma}|^2\right. \\
 &\quad \left.- 8\sqrt{\frac{3}{7}}D_{f\sigma}^*D_{p\sigma}\cos\Delta_{pf}\right),
 \end{aligned}$$

and

$$A_6'' = \pi\alpha h\nu\left(\frac{100}{33}|D_{f\sigma}|^2\right), \quad (3)$$

and for the perpendicular transitions by

$$\begin{aligned}
 A_0^\perp &= 2\pi\alpha h\nu(|D_{p\pi}|^2 + |D_{d\pi}|^2 + |D_{f\pi}|^2), \\
 A_2^\perp &= 2\pi\alpha h\nu\left(-|D_{p\pi}|^2 + \frac{5}{7}|D_{d\pi}|^2 + |D_{f\pi}|^2\right. \\
 &\quad \left.- 6\sqrt{\frac{2}{7}}D_{f\pi}^*D_{p\pi}\cos\Delta_{pf}\right), \\
 A_4^\perp &= 2\pi\alpha h\nu\left(-\frac{12}{7}|D_{d\pi}|^2 + \frac{3}{11}|D_{f\pi}|^2\right. \\
 &\quad \left.+ 6\sqrt{\frac{2}{7}}D_{f\pi}^*D_{p\pi}\cos\Delta_{pf}\right),
 \end{aligned}$$

and

$$A_6^\perp = 2\pi\alpha h\nu\left(-\frac{25}{11}|D_{f\pi}|^2\right). \quad (4)$$

In the above expressions,  $\alpha$  is the fine structure constant,  $D_{lm}$  represents the dipole matrix element for the transition into the  $\varepsilon lm$  state, and  $\Delta_{ll'}$  indicates the phase difference between  $\varepsilon l$  and  $\varepsilon l'$  partial waves. Although all quantities of  $D_{lm}$  and  $\Delta_{ll'}$  in Eqs. (3) and (4) can be determined by least-squares fitting Eq. (2) to the experimental data, there are possibilities yielding the meaningless values owing to the small number of the data points with not small error bars and without the definite value of the linear polarization degree. Therefore, we have determined the relative values for the expansion coefficients  $A_K$  of the Legendre polynomials by the least-squares fit. The

zero offset of the photoelectron ejection angle  $\theta$  was included in the fitting parameters within the acceptance angle of the ion detector. The expansion coefficients  $A_K$  obtained from the fitting procedure are given in Table I. The uncertainties in the values of  $A_K$  have been estimated less than 20%.

For the parallel transitions, a prominent increase of  $A_6''$  relative to  $A_0''$  is noticed at 419 eV where the shape resonance takes place. Since the expansion coefficient of  $A_6''$  is expressed by  $|D_{f\sigma}|^2$ , i.e., the square of the dipole matrix element related to the  $f$  partial wave [see Eq. (3)], the present results reveal directly that the shape resonance is caused in a single channel, i.e., the  $f$  component of the  $\sigma$  continuum wave functions [20]. According to the theoretical calculations based on the multiple scattering formalism, the resonance enhancement is caused by a centrifugal barrier acting on the  $f$  partial wave in the  $\sigma_u$  continuum of  $N_2$  [2]. Thus the theoretical interpretation for the origin of the shape resonance is for the first time confirmed directly by the present work. Although Dill, Siegel, and Dehmer [6] have calculated the fixed-molecule  $K$ -shell photoelectron angular distributions of  $N_2$  which are comparable with the present results, they have presented only the three dimensional plots of the angular distributions for the parallel and perpendicular transitions. Therefore, it is difficult to perform a detailed quantitative comparison between the present results and their calculations. It is obvious, however, that Dill, Siegel, and Dehmer [6] overestimated the contribution of the  $f$  component of the  $\sigma_u$  continuum wave function at the shape resonance.  $A_4'' < 0$  at 419 eV means that the interference term between  $f\sigma$  and  $p\sigma$  partial waves in Eq. (3) contributes significantly. For the angular distribution pattern at 412 eV in Fig. 1, a slightly increasing behavior at  $\theta \geq 50^\circ$  is observed. Taking the small contribution of  $A_6''$  into account, the  $d$  component of the  $\sigma_g$  continuum wave function may considerably contribute to the parallel transitions at 412 eV. A monotonically decreasing angular distribution with the increase of  $\theta$  is seen at 447 eV in Fig. 1. This angular distribution pattern may suggest not only the contribution of the  $s$ ,  $p$ ,  $d$ , and  $f$  components of the  $\sigma$  continuum wave functions but also the contribution of the higher  $l$  components ( $l \geq 4$ ) neglected here at higher photon energies.

TABLE I. Expansion coefficients  $A_K$  of the Legendre polynomials after normalization with  $A_0''$  and  $A_0^\perp$  giving the isotropic angular distributions.

Photon energy $h\nu$ (kinetic energy)	Parallel transitions $1s\sigma \rightarrow \varepsilon\sigma$				Perpendicular transitions $1s\sigma \rightarrow \varepsilon\pi$			
	$A_0''$	$A_2''$	$A_4''$	$A_6''$	$A_0^\perp$	$A_2^\perp$	$A_4^\perp$	$A_6^\perp$
412 eV ( $E_k = 2$ eV)	1.0	0.82	1.15	0.25	1.0	-0.16	-0.45	-0.02
419 eV ( $E_k = 9$ eV)	1.0	0.25	-0.22	1.01	1.0	-0.12	-0.47	-0.05
447 eV ( $E_k = 37$ eV)	1.0	1.86	0.37	0.49	1.0	-0.51	-0.23	-0.15

In contrast to the case of the parallel transitions, no increase of  $A_6^\perp$  relative to  $A_0^\perp$  is observed at 419 eV for the perpendicular transitions, as predicted theoretically by Dehmer and Dill [2]. The contribution of  $A_6^\perp$  is negligibly small at 412 and 419 eV, which is related to  $|D_{f\pi}|^2$ , the square of the dipole matrix element for the  $1s\sigma_g \rightarrow f\pi_u$  ionization channel. Then, if neglecting this contribution,  $A_2^\perp$  is proportional to  $-|D_{p\pi}|^2 + \frac{5}{7}|D_{d\pi}|^2$ , and  $A_4^\perp$  is proportional to  $-\frac{12}{7}|D_{d\pi}|^2$  [see Eq. (4)]. From these relations and the values of  $A_2^\perp$  and  $A_4^\perp$  given in Table I, it can be found that the intensity ratios of  $|D_{p\pi}|^2$  to  $|D_{d\pi}|^2$  are about 1.3 both at 412 and 419 eV. These results are consistent with the theoretical partial photoionization cross sections for the  $\pi_u$  and  $\pi_g$  channels by Dehmer and Dill [2]. However, Dill, Siegel, and Dehmer [6] overestimated the contribution of the  $f\pi_u$  component at 419 eV, which makes a peak of the angular distribution pattern at  $\theta = 90^\circ$ . The slight increase of  $A_6^\perp$  at 447 eV may suggest that the  $f$  partial wave component (and also  $l \geq 4$ ) starts to contribute slightly at this photon energy.

The  $A_K$  values determined by the present work are consistent with the asymmetry parameters  $\beta$  measured by Lindle *et al.* [21]. The relatively large values of  $A_6''$  and  $A_4^\perp$  at the  $\sigma^*$  shape resonance; i.e., roughly speaking, the large contributions of  $f\sigma_u$ , and  $d\pi_g$  partial waves are reflected in the large deviation [21] ( $\sim 0.75$ ) of the  $\beta$  parameter from the value of 2 expected for the pure  $p$  partial wave. At 447 eV the values of  $A_2''$  and  $A_2^\perp$  are relatively large; i.e., the large contributions of  $p\sigma_u$  and  $p\pi_u$  partial waves are expected at higher energies. This evaluation expects the  $\beta$  value close to 2 at higher energies. Indeed, the  $\beta$  value determined by Lindle *et al.* [21] is  $\sim 1.9$  at 439 eV.

In conclusion, we have for the first time measured the angular distributions of the  $1s\sigma$  photoelectrons from fixed-in-space  $N_2$  molecules via coincidence techniques. The present results on the angular distributions, providing a sensitive and direct probe of the molecular photoionization dynamics, have made the nature of the molecular  $\sigma^*$  shape resonance in the  $K$ -shell spectrum clear.

We would like to acknowledge Professor N. Kosugi and Professor F. Koike for their fruitful discussion and comments on theoretical treatment. We are grateful to the staff of the Photon Factory for the stable operation of the storage ring. This work has been performed under approval of the Photon Factory Advisory Committee (Proposal No. 93G311).

\*Permanent address: Institute for Molecular Science, Myodaiji, Okazaki-shi, Aichi-ken 444, Japan.

†Permanent address: The Institute of Physical and Chemical Research, 2-1 Hirosawa, Wako-shi, Saitama-ken 350-01, Japan.

- [1] For example, J. Stöhr, *NEXAFS Spectroscopy*, Springer Series in Surface Sciences Vol. 25 (Springer-Verlag, Berlin, Heidelberg, 1992).
- [2] J. L. Dehmer and D. Dill, *Phys. Rev. Lett.* **35**, 213 (1975); *J. Chem. Phys.* **65**, 5327 (1976).
- [3] D. Dill, *J. Chem. Phys.* **65**, 1130 (1976).
- [4] I. G. Kaplan and A. P. Markin, *Sov. Phys. Dokl.* **14**, 36 (1969).
- [5] J. W. Davenport, *Phys. Rev. Lett.* **36**, 945 (1976).
- [6] D. Dill, J. Siegel, and J. L. Dehmer, *J. Chem. Phys.* **65**, 3158 (1976).
- [7] A. V. Golovin, V. V. Kuznetsov, and N. A. Cherepkov, *Sov. Tech. Phys. Lett.* **16**, 363 (1990).
- [8] A. V. Golovin, N. A. Cherepkov, and V. V. Kuznetsov, *Z. Phys. D* **24**, 371 (1992).
- [9] H. Maezawa, Y. Suzuki, H. Kitamura, and T. Sasaki, *Appl. Opt.* **25**, 3260 (1986).
- [10] A. Yagishita, S. Masui, A. Toyoshima, H. Maezawa, and E. Shigemasa, *Rev. Sci. Instrum.* **63**, 1351 (1992).
- [11] E. Shigemasa, K. Ueda, Y. Sato, T. Sasaki, and A. Yagishita, *Phys. Rev. A* **45**, 2915 (1992).
- [12] A. Yagishita, H. Maezawa, M. Ukai, and E. Shigemasa, *Phys. Rev. Lett.* **62**, 36 (1989).
- [13] E. Shigemasa, K. Ueda, Y. Sato, T. Hayaishi, H. Maezawa, T. Sasaki, and A. Yagishita, *Phys. Scr.* **41**, 63 (1990).
- [14] A. Yagishita and E. Shigemasa, *Rev. Sci. Instrum.* **63**, 1383 (1992).
- [15] N. Kosugi, E. Shigemasa, and A. Yagishita, *Chem. Phys. Lett.* **190**, 481 (1992).
- [16] N. Kosugi, J. Adachi, E. Shigemasa, and A. Yagishita, *J. Chem. Phys.* **97**, 8842 (1992).
- [17] E. Shigemasa, T. Hayaishi, T. Sasaki, and A. Yagishita, *Phys. Rev. A* **47**, 1824 (1993).
- [18] A. Yagishita, E. Shigemasa, J. Adachi, and N. Kosugi, in *Proceedings of the 10th International Conference on Vacuum Ultraviolet Radiation Physics*, edited by F. J. Wuilleumier, Y. Petroff, and I. Nenner (World Scientific Publishing, Singapore, 1993), p. 201.
- [19] A. Yagishita, E. Shigemasa, and N. Kosugi, *Phys. Rev. Lett.* **72**, 3961 (1994).
- [20] D. Loomba, S. Wallace, D. Dill, and J. L. Dehmer, *J. Chem. Phys.* **75**, 4546 (1981).
- [21] D. W. Lindle, C. M. Truesdale, P. H. Kobrin, T. A. Ferrett, P. A. Heimann, U. Becker, H. G. Kerkhoff, and D. A. Shirley, *J. Chem. Phys.* **81**, 5375 (1984).